Plant Mol Biol (2009) 71:39–50
DOI 10.1007/s11103-009-9507-9

Over-expression of an AT-hook gene, *AHL22*, delays flowering and inhibits the elongation of the hypocotyl in *Arabidopsis thaliana*

Chaowen Xiao · Fulu Chen · Xuhong Yu · Chentao Lin · Yong-Fu Fu

Received: 16 January 2009 / Accepted: 24 May 2009 / Published online: 11 June 2009

Abstract The Arabidopsis genome encodes 29 AHL (AT-hook motif nuclear localized) proteins, but the function for most of them remains unknown. We report here a study of the *AHL22* gene, which was originally identified as a gain-of-function allele that enhanced the phenotype of the *cry1 cry2* mutant. AHL22 is a nuclear protein with the binding activity for an AT-rich DNA sequence. *AHL22* overexpression delayed flowering and caused a constitutive photomorphogenic phenotype. The loss-of-function *AHL22* mutant showed no clear phenotype on flowering, but slightly longer hypocotyls. However, silencing four *AHL* genes (*AHL22*, *AHL18*, *AHL27*, and *AHL29*) resulted in early flowering and enhanced *ahl22-1* mutant phenotype on the growth of hypocotyls, suggesting genetic redundancy of *AHL22* with other *AHL* genes on these plant developmental events. Further analysis showed that *AHL22* controlled flowering and hypocotyl elongation might result from primarily the regulation of *FT* and *PIF4* expression, respectively.

C. Xiao, F. Chen and X. Yu contributed equally to the work.

Electronic supplementary material The online version of this article (doi:10.1007/s11103-009-9507-9) contains supplementary material, which is available to authorized users.

C. Xiao · F. Chen · Y.-F. Fu (✉)
Institute of Crop Sciences, The National Key Facility for Crop Gene Resources and Genetic Improvement (NFCRI), Chinese Academy of Agricultural Sciences, Nandajie12, Zhongguancun, 100081 Haidian District, Beijing, People's Republic of China
e-mail: fuyf@caas.net.cn; fufu19cn@163.com

X. Yu · C. Lin (✉)
Department of Molecular, Cell & Developmental Biology, University of California, Los Angeles, CA 90095, USA
e-mail: clin@mcdb.ucla.edu

Keywords *Arabidopsis thaliana* · AT-hook · Flowering time · Hypocotyl · Photomorphogenesis

Introduction

The development of a plant is heavily dependent on its surroundings, and plants respond to environmental and endogenous signals by generating cellular signals which trigger cell- and development-specific patterns of gene expression. This response depends, as in other eukaryotes, on the organization of genomic DNA into chromatin, a process which comprises the first step in gene transcription (Bastow and Dean 2003; Sung and Amasino 2004). The AT-hook is a small DNA-binding motif, and has been shown to be present in a broad range of DNA-binding proteins, including high mobility group (HMG) proteins, homeodomains, bromodomains, and both PHD and zinc finger proteins. This group of proteins are mechanistically involved in both local and global changes in chromatin structure, and act to increase the structural flexibility of DNA via the promotion of the assembly of the nucleoprotein complex, which controls transcription (Harrer et al. 2004; Grasser et al. 2007a). The AT-hook motif proteins regulate gene expression through the interaction of the motif with the narrow minor groove of AT-rich DNA sequences. The HMGA and HMGB proteins appear to bind chromatin only transiently before moving on to the next site, and are implicated in a continuous genome scan for targets (Harrer et al. 2004; Launholt et al. 2006).

The AT-hook motif is characterised with the peptide sequence RGRP, with the flanking sequences of this motif determining its DNA-binding affinity, and thereby its function of the protein. Aravind and Landsman (1998) have recognized three types of such proteins. Type I proteins

have the highest affinity to DNA, as the C-terminal of their core RGRP carries an additional module composed of a number of basic residues, usually along with a glycine, which together form a supporting polar network and provide additional contacts with the target DNA. In addition to the AT-hook motif, plant members of this protein family also carry one PPC (plant and prokaryotic conserved) domain, the hydrophobic regions of which are essential for their nuclear localization (Fujimoto et al. 2004; Matsushita et al. 2007; Street et al. 2008). The AT-hook motif itself also contributes to nuclear localization, probably as a result of methylation of the arginine residue within the motif (Sgarra et al. 2006; Cattaruzzi et al. 2007).

There are many AT-hook proteins (containing AT-hook motif proteins) in plants identified from a range of species, including *Arabidopsis thaliana* (*At*), rice (*Oryza sativa*), maize (*Zea mays*), pea (*Pisum sativum*) and the Madagascar periwinkle (*Catharanthus roseus*). In *At*, they are referred to as AHLs (AT-hook motif nuclear localized proteins) (Fujimoto et al. 2004; Grasser et al. 2007b; Vom Endt et al. 2007). Their expression has been detected in most plant organs (Matsushita et al. 2007; Street et al. 2008). When transgenic GUS activity was driven by AT-hook promoters of *AHL27* and *AHL29*, expression was concentrated in the vascular system, and was not modulated by light (Street et al. 2008). AT-hook proteins have been shown to be involved in the maintenance of meristem identity (Su et al. 2006), leaf longevity (Lim et al. 2007), photomorphogenesis and the development of flowers and leaves (Street et al. 2008), the jasmonate signal pathway (Vom Endt et al. 2007) and gibberellin homeostasis (Matsushita et al. 2007). These observations suggest that the AT-hook genes play multiple roles in plant development, although single *AHL* mutants, such as the loss-of-function mutant of *AHL27* (At1g20900), have apparently no observable phenotype with respect to either seedling or adult plant morphology. A double mutant of *AHL27* and *AHL29* (At1g76500), two genes which are closely related to each other, flowered at the same time as the wild type. However, under low levels of illumination, seedlings of the double mutant produced longer hypocotyls than either the wild type or either of the single mutants. These observations imply a level of redundancy among the *AHL* genes, and that the various functions of a particular AHL protein are arrived at via distinct mechanisms. In contrast to the loss-of-function mutants, dramatic phenotypic changes are induced when various *AHL* genes are transgenically over-expressed (Su et al. 2006; Lim et al. 2007; Street et al. 2008).

The plant cryptochromes encoded by *CRY1* (Ahmad and Cashmore 1993; Lin et al. 1996) and *CRY2* (Lin et al. 1998) are the major receptors of blue light, and are involved in the control of numerous developmental events, including the determination of flowering time and hypocotyl growth. Compared to the wild type, the flowering of the *cry2* mutant is much delayed under long, but not under short day conditions (Guo et al. 1998; El-Din El-Assal et al. 2003), while mutations at *CRY1* largely affect hypocotyl growth (Ahmad and Cashmore 1993; Lin et al. 1996). The double mutant *cry1 cry2* flowers later and has longer hypocotyls than either of the single mutants (Mockler et al. 1999).

Activation tagging is a gain-of-function mutagenesis method which permits the identification of genes involved in a given process, and the phenotypes conferred by the over-expression of these genes can be informative as to the function of the tagged genes (Weigel et al. 2000). We describe here the screening of an activation tagged library in background of the *cry1 cry2* double mutant, which led to the identification of a late-flowering individual. We show that this phenotype is the outcome of *AHL22* (At2g45430, an AT-hook gene) over-expression, and that *AHL22* affects on hypocotyl growth either.

Methods

Gene cloning and plasmid construction

Activation-tagging mutagenesis was performed in a *cry1 cry2* mutant background as (Weigel et al. 2000; Zhao et al. 2007) did. The mutants with flowering phenotype were screened, and one of later flowering mutant, *ecc* (*enhancer of cry1 cry2*) *2*, was identified. With the results of Tail-PCR (Weigel and Glazebrook 2002), *ecc2* carried a T-DNA which inserted in the upstream of At2g45430. Using genomic sequences from the TAIR8 database (http://www.arabidopsis.org/), the full-length *AHL22* open reading frame was amplified by PCR with primers (see Table S1) containing appropriate restriction sites, and the amplicon was cloned into the 35SpBARN (LeClere and Bartel 2001) and pEGAD vectors (Cutler et al. 2000) to obtain the binary vectors p*35S::AHL22* and p*35S::GFP:AHL22*. The open reading frame of *AHL18* (At3g60870) was cloned into pLeela vector using Gateway system (Invitrogen) to obtain the binary vector p*35S::AHL18*. The special fragment sequences of *AHL22* and *AHL18* were combined using overlap PCR (Lu 2005), and cloned into pJawohl8 to obtain the *AHL22-AHL18* double RNAi construct. With the same approach, the quadruple RNAi vector of *AHL22*, *AHL18*, *AHL27* and *AHL29* was constructed. Sequence alignment was performed using MEGA v3.1.

Plant materials and growth conditions

Arabidopsis thaliana seeds were pretreated at 4°C for 3 days and grown at a constant temperature of 22°C under

various lighting regimes. For hypocotyl measurement, the long day regime was 16 h light 80 μmol m^{-2} s^{-1} and 8 h dark, the short day regime 8 h light 100 μmol m^{-2} s^{-1} and 16 h dark, continuous blue light 6 μmol m^{-2} s^{-1}, continuous red light 30 μmol m^{-2} s^{-1}, continuous far-red light 0.6 μmol m^{-2} s^{-1}. *At* plants were agroinfected with *Agrobacterium tumefaciens* strain GV3101 MP90 and pGV3101 MP90RK, using the floral dipping method (Clough and Bent 1998). Flowering time data were measured on the basis of the number of rosette and cauline leaves formed by the primary meristem and days to flower, and represent the mean of at least 16 per each line. T-DNA insertion lines of Salk_018866 and Salk_143279 were obtained from ABRC. PCR based genotyping used primers recommended by http://signal.salk.edu/tdnaprimers.2.html.

Electrophoretic mobility shift assay

The open reading fragments encoding the AHL22 and AHL27 full-length proteins were cloned into the entry clone pDONR201 (Invitrogen), and recombined into the destination vector pDEST17 (Invitrogen). Expression of the His-AHL22 and His-AHL27 fusion proteins was induced by 1 mM IPTG (Sigma) in *E.coli* strain BL21-star. After four additional hours at 28°C, the bacterial cells were harvested by centrifugation at 10,000*g* for 15 min at 4°C, and resuspended in 20 ml of EXB buffer [50 mM Sodium Phosphate (pH 8.0), 300 mM NaCl, 1 mM *β*-mercaptoethanol, and 1 mM phenylmethylsulfonyl fluoride (PMSF), 10 mM Imidazole, 8 M Urea]. The cells were disrupted by sonication and the supernatants were obtained by centrifugation at 16,000*g* for 30 min at 4°C. The soluble fraction was incubated with Ni-NTA Agarose Beads (Qiagen) with shaking for 1 h, and then applied into a purification column and washed two times using the EXB buffer. Finally the His-tagged protein was eluted by five bed-volumes of ELB buffer [50 mM Sodium Phosphate (pH 7.0), 300 mM NaCl, 200 mM Imidazole, 8 M Urea].

An electrophoretic mobility shift assay was performed using LightShift Chemi-luminescent EMSA kits (Pierce). The 39-bp synthetic oligonucleotide (5′-TAACAC**ATATTTT**GATAA**ATTTATT**ACTAAAAC**TATTTT**-3′)(bold letters indicate A/T rich motif; Lim et al. 2007) was used as a probe. Competition experiments using the wild-type competitor and mutated competitors (5′-TAACACA**CTGCAG**GATAAATTTATTACTAAAACTATTTT-3′) (bold letters indicate mutated sites) were also performed. The probes were labeled with biotin 3′-end DNA labeling kit (Pierce) according to the instruction. Briefly, binding reactions containing 10 μg of His-tagged proteins and 1 nmol of oligonucleotide were performed for 30 min in binding buffer [2.5% glycerol, 0.05% Nonidet P-40, 50 mM KCl, 5 mM $MgCl_2$, 1 mM EDTA, 10 mM Tris, pH 7.6, and 50 ng of poly(dI-dC)]. Protein-nucleic acid complexes were resolved using a nondenaturating polyacrylamide gel consisting of 6% acrylamide, and transferred to a nylon membrane. The membrane was incubated in blocking solution followed by incubation with streptavidin-peroxidase. After extensive washing, signal was detected with chemiluminescence solution.

Measurement of hypocotyl length

Arabidopsis thaliana seeds were surface-sterilized and sown on MS medium (0.5 g l^{-1} MES pH 5.7 and 0.8% w/v agar). The seeds were held at 4°C for 3 days, exposed to white light for 4 h to stimulate germination, and then cultured for 6 or 8 days at 22°C under various light and photoperiod conditions to measure the hypocotyl length. The length of hypocotyl was measured to an accuracy of 0.5 mm (Lin et al. 1998; Mockler et al. 1999).

GUS staining

A 2.3 kbp fragment upstream of the *AHL22* coding sequence was cloned from the genomic DNA of the Columbia ecotype, and fused to the *GUS* report gene to form a binary vector using the GATEWAY cloning system (Invitrogen). The *GUS* fusion gene was introduced into Columbia, and T2 lines were used for analysis. For GUS staining, plant tissue was immersed in a buffer composed of 50 mM sodium phosphate pH 7.0, 2 mM potassium ferricyanide, 2 mM potassium ferrocyanide, 0.2% v/v Triton X-100 and 2 mM 5-bromo-4-chloro-3-indolyl-beta-D-glucuronic acid, cyclohexylammonium salt and held at 37°C overnight. The material was decoloured in ethanol:acetic acid (3:1, v/v) and analysed by light microscopy (Nikon SMZ1000, Japan).

Subcellular localization of GFP-AHL22 in *Arabidopsis thaliana*

GFP (green fluorescent protein) was monitored in guard cells, hypocotyl and root cells of 3-day-old *35S::GFP:AHL22* seedlings grown on MS medium by confocal microscopy (LEICA TCS SP2, Germany). GFP fluorescence was induced by exposure to blue light.

Semi-quantitative RT-PCR and quantitative real-time RT-PCR

Total RNA was extracted from 10-day-old seedlings and different organs using Trizol reagent (Invitrogen). The samples were treated with RQ1 RNase-free DNase (Promega) to remove any contamination with genomic DNA. RNA quality was verified by agarose gel electrophoresis,

and first-strand synthesis was performed with an oligo(dT_{17}) primer (Fermentas), following the manufacturer's instructions. The constitutively expressed *ACT2* was used as an internal control. Quantitative real-time RT-PCR was performed following the StepOne Real-Time PCR system (Applied Biosystems). Data were analysed using StepOne software (ABI, Applied Biosystems) and transcript levels were calculated relative to the transcript level of *ACT2*. The sequences of the primers used for semi-quantitative RT-PCR and quantitative real-time RT-PCR are listed in Table S1.

Results

The over-expression of *AHL22* delays flowering in long days and short days

One activation-tagging mutant, *ecc* (*enhancer of cry1 cry2*) *2* with late-flowering phenotype, was identified from the background of *cry1 cry2* double mutant. After genotyping (Weigel and Glazebrook 2002), it was confirmed that the phenotype of *ecc2* may result from overexpression of an AT-hook gene, *AHL22* (At2g45430). But the *ecc2* plants were sterile and no seeds were got from them. So, *AHL22* was cloned from the wild type plants (ecotype Columbia) using RT-PCR, with primers based on the genomic sequence of At2g45430. The protein sequence shows that *AHL22* is an intron-less gene encoding a 317 residue peptide. Its protein has a single AT-hook motif and a conserved PPC domain (Fig. S1A). Its characters of motif and its flanking sequence is typical of type I proteins, as described by Aravind and Landsman (1998).

Then *AHL22* gene driven by the cauliflower mosaic virus (CaMV) 35S promoter was expressed in the background of wild type COL. In all, 36 independent transgenic lines were obtained and classified on the basis of phenotype (flowering time and fertility) into three types (Fig. S1B). Type I plants (6 out of 36) took 150 days to reach flowering under long days, and were branchy and sterile (Fig. S1C); in these plants the level of *AHL22* mRNA was maintained at a high level (Fig. S1D). Type II plants (6 out of 36) flowered later than the wild type, but earlier than type I, and were partially sterile—in these, the level of *AHL22* mRNA was moderate (Fig. S1D). Although *AHL22* transcript in type III plants (24 out of 36) was more abundant than in the wild type (Fig. S1D), the flowering time and fertility of these plants were indistinguishable from that of the wild type. Thus the expression level of *AHL22* was correlated with phenotype. Type I plants resembled the *ecc2* mutant, suggesting that the over-expression of *AHL22* was responsible for the *ecc2* mutant phenotype. In a more detailed study of the function of *AHL22* on plant development, the type II plants were used—these were hereafter referred to as over-expressing-*AHL22* (*AHL22*ox) plants. *AHL22*ox plants flowered later than the wild type under both long day and short day conditions, and the total number of leaves was more than triple in short days than that in long days (Fig. 1A, Ea), suggesting that *AHL22*ox was still sensitive to photoperiod.

AHL22 involves in flowering regulation by redundant function with other *AHL* genes

To analyze the function of *AHL22*, we ordered two mutant lines of *AHL22* gene of Salk_018866 (*ahl22-1*) and Salk-143279 (*ahl22-2*) from ABRC (http://www.arabidopsis.org/). There was no transcripts amplified from *ahl22-1* allele, but *AHL22* mRNA was clearly detected in *ahl22-2* line (Fig. 1Eb, S2), suggesting that *ahl22-1* was a null mutant. The *ahl22-1* mutant, however, reaches flowering at nearly the same time as do the wild type plants (Fig. 1B), suggesting functional redundancy exists between *AHL22* and other genes. Another *AHL* gene, *AHL18*, may be the candidate, since *AHL18* is in the same phylogenetic clade of *AHL22* (Fujimoto et al. 2004). Therefore, RNAi plants silencing both *AHL18* and *AHL22* genes were constructed, and plants showed a decreased expression of *AHL22* and *AHL18* (Fig. 1Ec). Unexpectedly, no clear flowering phenotype was observed in these plants (Fig. 1C). However, plants of overexpression of *AHL18* (*AHL18*ox) had similar phenotype (late flowering) to that of *AHL22*ox (Fig. S3). The results suggested that there were more genes involved in the network of flowering regulation of *AHL22*.

Because overexpression of *AHL27* is known to delay flowering time (Weigel et al. 2000) and *AHL29* is the gene closest to *AHL27*, *AHL27* and *AHL29* may be the candidates with the redundant function of flowering regulation with *AHL22*, even though a double mutant *ahl27 ahl29* flowered at the same time as the wild type (Street et al. 2008). The proteins of four AHLs share highly conserved sequences (Fig. S1A). Therefore, we constructed *AHL18-AHL22-AHL27-AHL29* quadruple genes silencing plants. Interestingly, the quadruple silencing plants displayed obviously early flowering phenotype (Fig. 1D), even though the transcripts of all of these four genes were not completely knocked out (Fig. 1Ed). The results suggest that these four *AHL*s have a redundant role of flowering regulation even though *AHL22* has a very low level of transcripts in leaves as indicated below.

The over-expression of *AHL22* inhibits hypocotyl growth in a light-independent manner

Hypocotyl elongation, cotyledon opening, hook opening and plant greening are important events in photomorphogenesis. In *AHL22*ox plants, photomorphogenesis is

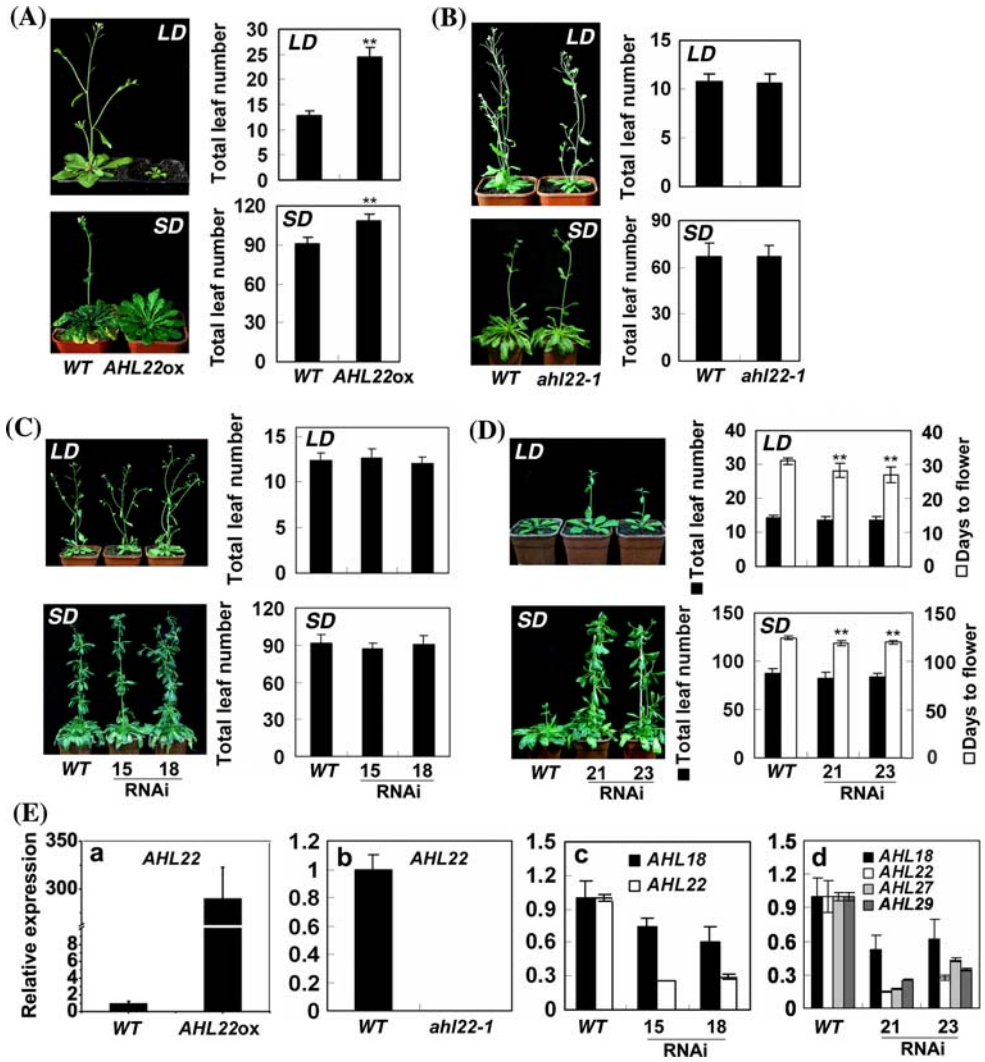

Fig. 1 The flowering phenotypes of *AHL22*ox and mutants. **A** Flowering phenotype of *AHL22*ox plants was delayed under both long day (*LD*) and short day (*SD*) conditions. **B** The *ahl22-1* mutant flowered at the same time as the wild type plants (*WT*) under both long and short day conditions. **C** The flowering time of *AHL18 AHL22* double RNAi plants under both long and short day conditions (15 and 18: two independent transgenic lines). **D** The flowering time of *AHL18-AHL22-AHL27-AHL29* quadruple RNAi plants under both long and short day conditions (21 and 23: two independent transgenic lines). The *right panel* of **A**, **B**, **C**, and **D** shows the number of rosette and cauline leaves and days at flowering. *Error bars* indicate standard deviation, every phenotype has at least 16 plants. Data in (**A**, **B**, **C**, **D**) were analyzed statistically using the *t*-test and a *double asterisk* indicates significance at $P < 0.01$ level. **E** mRNA expression level of *AHL22*, *AHL18*, *AHL27* and *AHL29* in different plants determined by quantitative real-time PCR. *Error bars* represent the standard deviation ($n = 3$). The labels of plants are the same as in **A**, **B**, **C**, and **D**

constitutively expressed (Fig. 2A). Regardless of growth conditions (dark, different photoperiods and different lights), *AHL22*ox plants produced short hypocotyls, and displayed an open hook and open cotyledons. This combination of traits is reminiscent of the phenotype of *constitutive photomorphogenic* (*cop*) (Osterlund et al. 2000; Saijo et al. 2003), *long hypocotyl5* (*hy5*) (Ulm et al. 2004). Compared to the wild type, *AHL22*ox photomorphogenesis suggests a response to variation in photoperiod and light quality. Red light and short days had a stronger effect than either blue light or long days (Fig. 2B), indicating that photoreceptors and the circadian clock could be involved in the process regulated by *AHL22*. Furthermore, *AHL22*ox displayed the same phenotype even in the absence of light. However, the *ahl22-1* mutant had slightly longer hypocotyls than the wild type in dark, long day and short day conditions (Fig. 2C, D), and the quadruple RNAi mutant had much longer hypocotyls than the wild type in different light conditions (Fig. 2E, F). The results suggest the function of *AHL22* in both photomorphogensis and skotomorphogenesis.

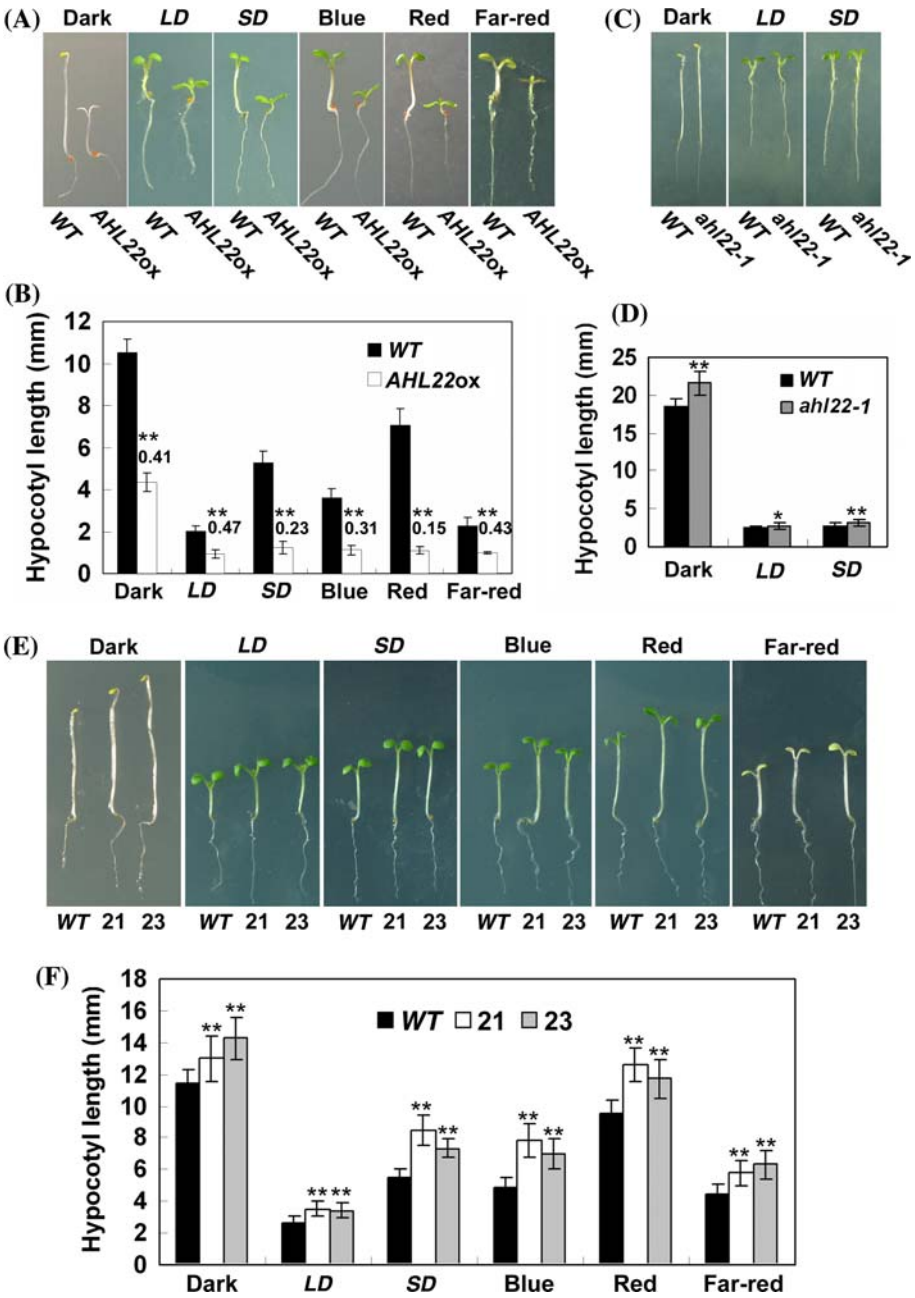

Fig. 2 *AHL22* affects hypocotyl elongation under various light conditions. **A** The hypocotyls of 6-day-old the wild type plants (*WT*) and *AHL22*ox seedlings under continuous darkness (*Dark*), long day (*LD*), short day (*SD*), continuous blue light (*Blue*), continuous red light (*Red*) and continuous far-red light (*Far-red*). **B** Quantitative analysis of the samples in **A**. The *digits* at the *top* of the *empty bar* show the ratio of hypocotyl length of *AHL22*ox to wild type under the same light regime ($n > 20$). **C** The hypocotyls of 8-day-old the wild type plants (*WT*) and *ahl22-1* mutant grown under continuous darkness, long days and short days. **D** Quantitative analysis of the samples in **C** ($n > 20$). **E** Hypocotyl phenotypes of 6-day-old *AHL18-AHL22-AHL27-AHL29* quadruple RNAi plants in different conditions. **F** Quantitative analysis of the samples in **E** ($n > 30$). Data in (**B**, **D**, **F**) were analysed statistically using the *t*-test. A *single asterisk* indicates significance at $P < 0.05$ and a *double asterisk* indicates significance at $P < 0.01$

The effect of *AHL22* over-expression on the expression of genes related to flowering and photomorphogenesis

To study the mechanism of AHL22 on flowering and hypocotyl growth, the expression of genes involved in the determination of flowering time and the development of the hypocotyl was monitored. *AHL22*ox plants showed lower levels of *CONSTANS* (*CO*) and *FLOWERING LOCUS T* (*FT*) transcripts than the wild type plants, while the expression levels of *SUPPRESSOR OF OVEREXPRESSION OF CONSTANS 1* (*SOC1*), *FLOWERING LOCUS C* (*FLC*) and *LEAFY* (*LFY*) were not measurably affected (Fig. 3). The reduced expression of *CO* and *FT* was independent of sampling time during the diurnal cycle, suggesting that both may be implicated in *AHL22* signalling. The flower identity gene *SEPALLATA3* (*SEP3*) is known to interact with *AP1*/*FUL*, and its over-expression to hasten flowering (Pelaz et al. 2001; Ferrario et al. 2003). In *AHL22*ox plants, the expression of *SEP3* was reduced (Fig. 3), indicating that the function of *AHL22* may require the participation of *SEP3*. On the contrary, the mRNA expression level of *FT* was upregulated in the *AHL18-AHL22-AHL27-AHL29* quadruple RNAi seedlings (Fig. S4).

Among the genes related to hypocotyl growth, the expression of various members of the *COP* (Osterlund et al. 2000; Saijo et al. 2003) and *PIF* (Ni et al. 1998; Huq

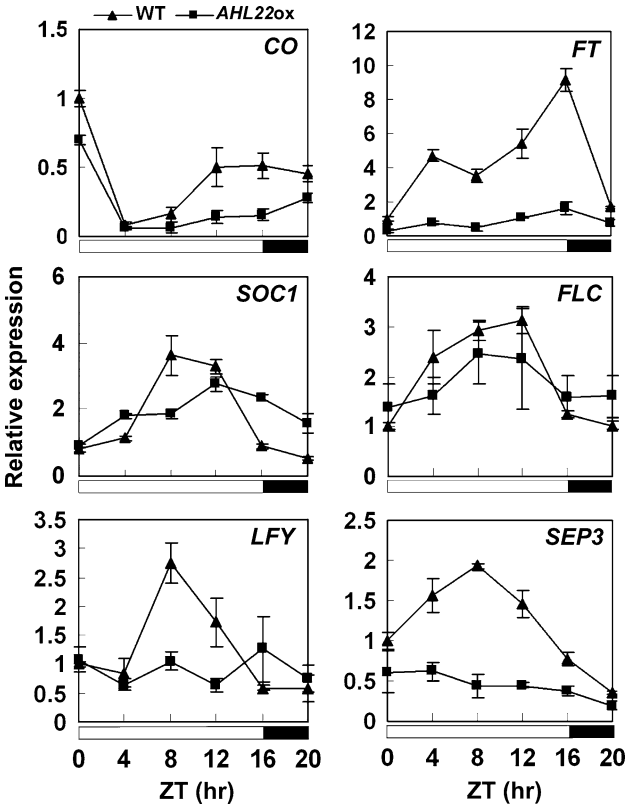

Fig. 3 The effect of *AHL22* over-expression on the transcription of *CO*, *FT*, *SOC1*, *FLC*, *LFY* and *SEP3*. Ten-day-old the wild type and *AHL22*ox seedlings were harvested every 4 h during a long day, and mRNA expression level was determined by quantitative real-time RT-PCR. *Error bars* represent the standard deviation ($n = 3$). *ZT* Zeitgeber

and Quail 2002) families, *CRY1* and *CRY2* (Ahmad and Cashmore 1993; Lin et al. 1996), *phyA* and *phyB* (Nagy and Schafer 2002) and *HY5* (Ulm et al. 2004) was determined (Fig. 4). The only ones of these genes showing a significantly reduced level of expression were *PIF3* and *PIF4*. Although the *AHL22*ox photomorphogenesis phenotype is reminiscent of that of various *cop* mutants, the only family member showing an expression level difference between the wild type and *AHL22*ox is *COP1*. However, this change is thought to be unrelated to the *AHL22*ox phenotype, since *AHL22* over-expression increased, rather than decreased *COP1* transcript abundance. The expression of neither *HY5* nor any of the photoreceptors was substantially altered. As expected, the mRNA expression level of *PIF4* was upregulated in the *AHL18-AHL22-AHL27-AHL29* quadruple RNAi seedlings (Fig. S4).

The tissue specific expression patterns of *AHL22*

A ~2.3 kb fragment upstream of the *AHL22* start codon was fused to a GUS reporter gene, and the resulting construct was transformed into the wild type plants to produce a set of 24 independent *AHL22::GUS* lines. GUS activity in these transgenic plants showed that expression of *AHL22* was concentrated at the hypocotyl-root transition zone and the root hair zone. Some weak GUS activity was present in the vascular system, but no signal was observed in young leaves (Fig. 5A). A semi-quantitative RT-PCR and a quantitative real-time RT-PCR analysis confirmed the in situ localization result. The level of transcripts in the leaf was below the level of detection of standard RT-PCR, even after 40 amplification cycles (data not shown), but was finally detected by nested RT-PCR (Fig. 5B). However, strikingly, over 1,000-fold more transcript was detected in the root compared to that present in the leaf (Fig. 5C). After the root, the inflorescence showed the next highest level of *AHL22* expression. So *AHL22* is a ubiquitously expressed gene even though it has different transcriptional levels in different organs.

AHL22 is a nuclear localized AT-hook protein

AHL proteins may be transcriptional factors which function in nucleus. To detect the localization of the AHL22 protein, *35S::GFP:AHL22* construct was instructed into wild type plants mediated by *Agrobacterium*. The plants over-expressing *GFP:AHL22* showed late flowering phenotype as the *AHL22*ox plants did (Fig. S5), suggesting that *GFP:AHL22* is functional. The sub-cellular localization of *AHL22* protein analyzed by confocal microscopy revealed clearly the nuclear localization of GFP:AHL22 protein in various organs (Fig. 6A), supporting that AHL22 may function in nucleus.

According to the classification of Aravind and Landsman (1998), AHL22 belongs to type I of AHL proteins. AHL22 protein has a single RGRP motif, and there is a glycine at the second position downstream of this motif and an extended module at the C-terminal of RGRP which includes basic residues forming a supporting polar network and additional contacts with DNA. These characters may confer to AHL22 protein high affinity of binding DNA. To detect this, an electrophoreticmobility shift assay (EMSA) was carried out with the A/T-rich DNA sequence from the promoter of the pea (*Pisum sativum*) *PRA2* gene (Lim et al. 2007). As shown in Fig. 6B, the AHL22 protein was able to bind to biotin-labeled oligonucleotide (lane 3) as AHL27 did (lane 2, Lim et al. 2007), and this binding affinity could be greatly decreased by competitor DNA fragment (unlabled) with the same wild-type sequence (lane 6). However, different from AHL27 protein, AHL22 could also bind to the mutated sequence (lane 3 and 5), suggesting AHL22 may have different binding specificity from AHL27 because the A/T-rich DNA sequence employed in this study has three A/T-rich motif (see "Methods" section,

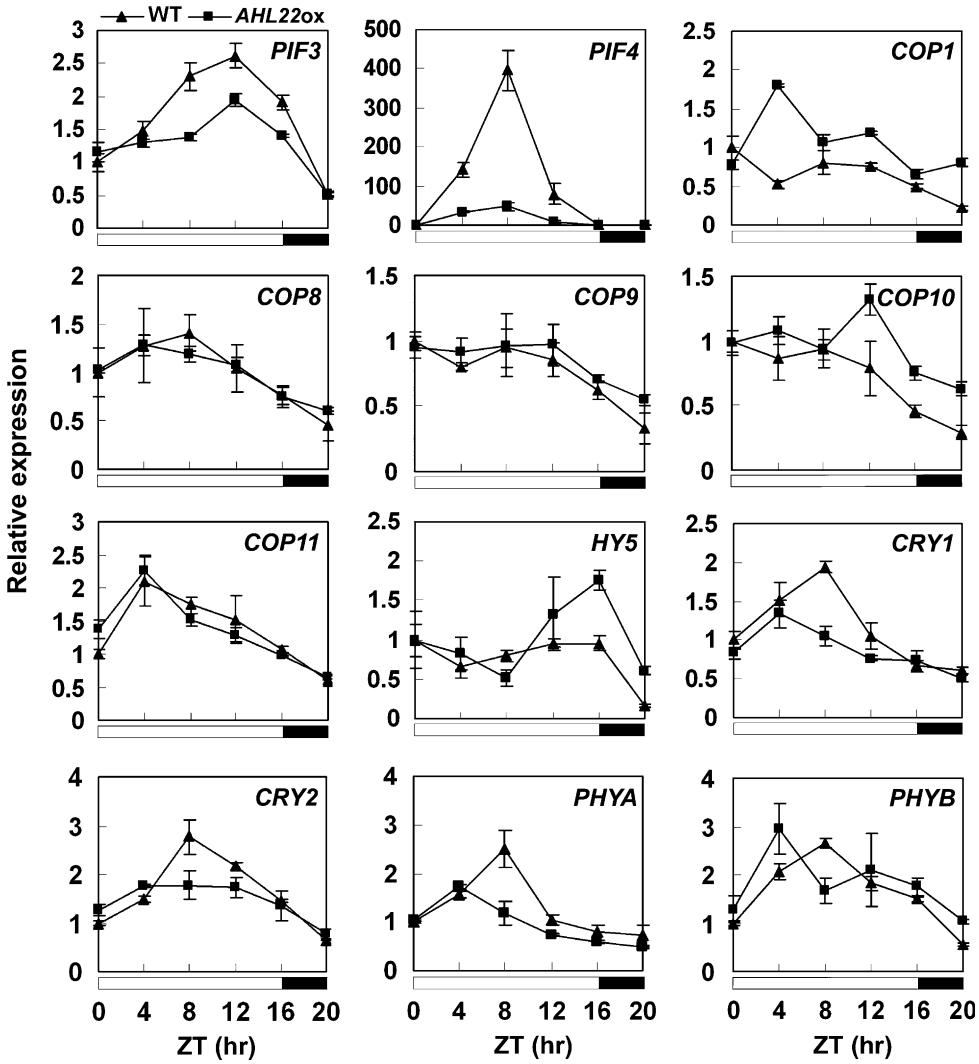

Fig. 4 Shorter hypocotyls in *AHL22*ox plants may be caused by induction of *PIF3* and *PIF4* expression. The diurnal variation in transcript level of *PIF3*, *PIF4*, *COP1*, *COP8*, *COP9*, *COP10*, *COP11*, *HY5*, *CRY1*, *CRY2*, *PHYA*, and *PHYB* in 10-day-old wild type and *AHL22*ox seedlings grown under long days, as detected by quantitative real-time RT-PCR. *Error bars* represent the standard deviation ($n = 3$). *ZT* Zeitgeber

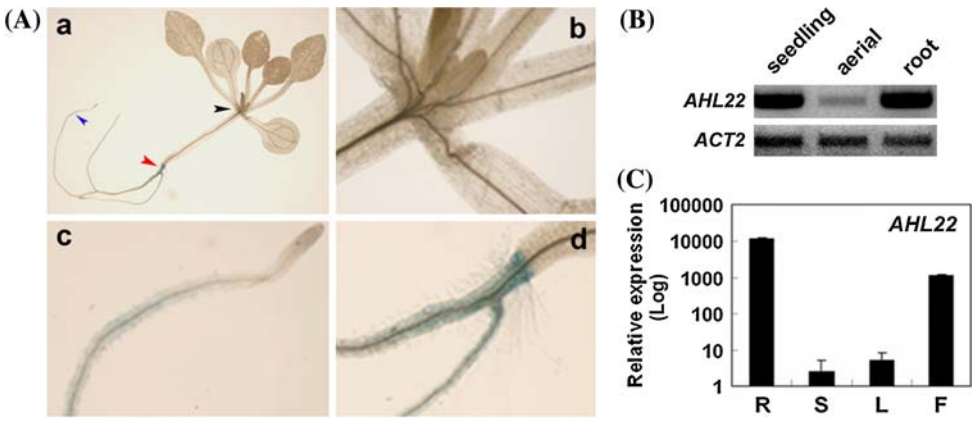

Fig. 5 Tissue-specific expression of *AHL22*. **A** GUS activity in *AHL22::GUS* transgenic seedlings grown under long days. *a* 14-day-old whole seedlings. The *black*, *blue* and *red arrows* indicate the focus for the close-up images displayed in (*b*) the meristem, (*c*) and (*d*) the root. **B** Nested RT-PCR profiles detected *AHL22* transcript in leaves of 10-day-old seedlings, *ACT2* was acted as control gene. **C** The *AHL22* mRNA level relative to *ACT2* in various organs of the wild type *WT*, as detected by quantitative real-time RT-PCR, the relative expression was showed using Log value. *R* root, *S* stem, *L* leaf, *F* flower. *Error bars* represent the standard deviation ($n = 3$)

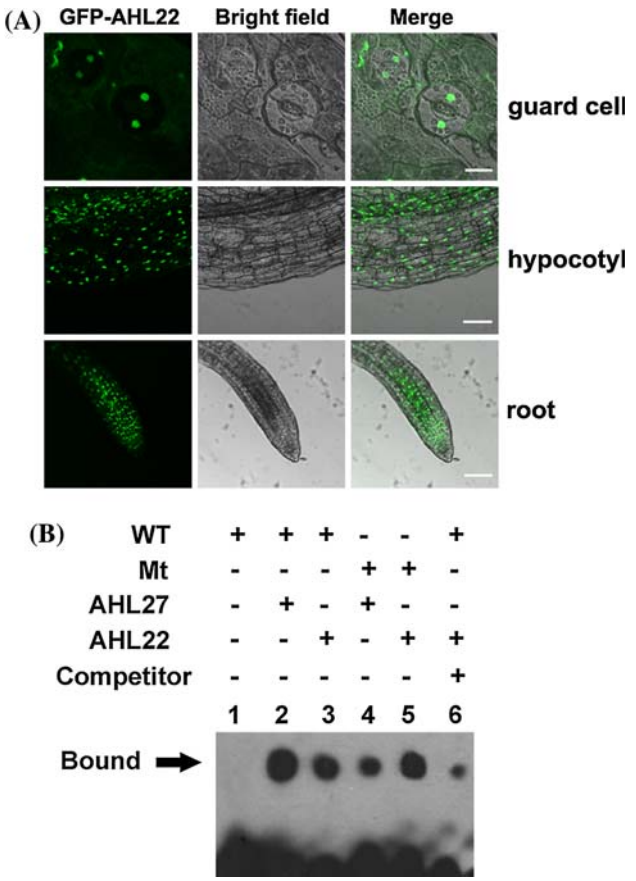

Fig. 6 AHL22 as a nuclear-localized AT-hook-binding protein. **A** Nuclear localization of AHL22. Confocal images showed the presence of GFP in guard cells, hypocotyls, and roots of 3-day-old *35S::GFP:AHL22* seedlings (Leica). *Left panels*, fluorescence image of GFP–AHL22; *middle panels*, bright field image; *right panel*, merged fluorescence image of GFP–AHL22 and bright field image. *Upper panels*, guard cells; *middle panels*, hypocotyl cells; *lower panels*, root cells. **B** Binding of AHL22 to an AT-rich oligonucleotide. The oligonucleotide sequence corresponds to a part of the AT-rich sequence present in the promoter of the pea *PRA2* gene. AHL27 protein was used as positive control (Lim et al. 2007). The 39-bp oligonucleotides of wild-type *WT* or mutant *Mt* were labeled with biotin for chemiluminescent detection. Competition experiment was carried out using the unlabeled wild-type oligonucleotide. The *arrow* indicates the location of the protein-bound, biotin labeled oligonucleotide

bold letters). Thus, AHL22 is a nuclear-localized protein which may bind to A/T-rich DNA sequence.

Discussion

AHL22 is a highly conserved and nuclear localized AT-hook protein

Members of the AT-hook protein family are thought to connect the nuclear framework with the MAR sequences in interphase nuclei, and to coat the chromosomes during mitosis (Fujimoto et al. 2004). The *At* genome contains 29 AT-hook protein paralogs, one of which, AHL22, is the type I sequence (Aravind and Landsman 1998). The C-terminal flanking sequence of the AHL22 RGRP motif contains basic lysine residues, which are able to form a supporting polar network and to promote additional contacts with DNA. The PPC domain of AHL22 may be important for its nuclear localization (Fig. 6, S1). Several lines of evidence show that AHLs have transcriptional activity (Fujimoto et al. 2004; Matsushita et al. 2007; Street et al. 2008), and we have demonstrated here that the expression level of a number of genes is altered in *AHL22*ox plants and RNAi plants (Fig. 3, 4, S4). Further evidence confirmed that AHL22 protein is a nuclear localized protein and can bind to A/T rich DNA sequence (Fig. 6). Thus, AHL22 protein may regulate flowering and the growth of hypocotyls with its transcriptional activity.

AHL22 may have a role of flowering regulation and hypocotyl elongation

AHL22 appears to be functionally redundant with other *AHL* genes, because the single mutant reaches flowering at almost the same time as does the wild type. There are at least three candidates from the information of bioinformatics (Fujimoto et al. 2004) and literature (Street et al. 2008): *AHL18*, *AHL27*, and *AHL29*. However, both the *ahl27 ahl29* double mutant (Street et al. 2008) and RNAi plants silencing both *AHL22* and *AHL18* (Fig. 1C) did not show early-flowering phenotype. Interestingly, the plants of silencing *AHL18*, *AHL22*, *AHL27*, and *AHL29* four genes obviously flowered earlier (Fig. 1D) and had higher transcripts of *FT* (Fig. S4) than the wild type did. Thus, their gene products may all represent proteins having functional redundancy with AHL22, and *AHL22* regulates flowering in deed through *FT* pathway, even though the mRNA level of *AHL22* in leaves is very low (Fig. 5) and single gene loss-of-function mutation (*ahl22-1*) does not produce marked alterations in flowering (Fig. 1B). We propose that in vivo, the AHLs are present at only a low level in leaves and function redundantly, and that ectopic over-expression disrupts the balance among the AHLs, with knock-on effects on plant development. Alternatively, *AHL22* may regulate flowering from roots. In this case, the high level of *AHL22* in roots may confer to the regulation of flowering.

In case of hypocotyl elongation, *AHL22* may have much stronger effect on it than its effect on flowering regulation, because *ahl22-1* mutant shows obviously longer hypocotyl phenotype. This phenotype is more obvious in *AHL18-AHL22-AHL27-AHL29* quadruple RNAi silencing plants, suggesting that these four genes function redundantly on hypocotyl development either. This conclusion is also supported by previous results in which *ahl27* and *ahl29*

mutants have longer hypocotyls (Street et al. 2008). From our results, *AHL22* may control hypocotyl elongation mainly dependent on the activity of *PIF4*.

Overexpression of *AHL22* has a pleiotropic effect on plant development

AHL27 is known to regulate flowering time, leaf longevity, and hypocotyl growth (Weigel et al. 2000; Lim et al. 2007; Street et al. 2008). The phenotype of *AHL22*ox plants differed in many ways including flowering and growth of hypocotyl from that of the wild type. *AHL22*ox plants also showed some different phenotypes in other developmental events including the growth of stem, roots and leaves, sterility, and greening (data not shown). Some of these differences were dependent on the light regime under which the plants were raised. Thus, like other *AHL* genes, it seems plausible that *AHL22* regulates a number of disparate developmental events via a range of mechanisms. The delayed flowering of *AHL22*ox is dependent on the ambient photoperiod, and is more pronounced under long days than that under short days. This suggests that the biological clock in *AHL22*ox plants is still operational and that it controls the function of *AHL22*. *CO*/*FT* lies at the core of a flowering promotion pathway which responds to photoperiod (Turck et al. 2008). The significant changes in expression level of *CO* and *FT* in *AHL22*ox plants (Fig. 3) are evidence that *AHL22* regulates flowering through these genes.

Rice PF1 is able to bind oat *phyA* and thereby enhance its activity, which has been taken to imply a regulatory role for AT-hook proteins in photomorphogenesis (Martinez-Garcia and Quail 1999). PIF3 and PIF4 proteins bind selectively to the biologically active form of *phyB* or *phyA* and function specifically in a branch of the *phyB* signalling network which regulates a subset of genes involved in cell expansion (Ni et al. 1999; Huq and Quail 2002). One of main regions of *AHL22* activity is in the hypocotyl-root transition zone (Fig. 5), suggesting a function associated with hypocotyl elongation. The over-expression of *AHL22* inhibits hypocotyl growth, irrespective of photoperiod or light quality, although short days and red light have a rather stronger effect than long days and blue light do (Fig. 2A, B). This behaviour mimics that of *cop* (Osterlund et al. 2000; Saijo et al. 2003) and *pif* (Ni et al. 1998; Huq and Quail 2002) mutants, but the expression of these genes (Fig. 4) implies that *AHL22* regulates hypocotyl growth through neither *COP* nor photoreceptors, but via *PIF3* and *PIF4*. It is also supported that *pif3* and *pif4* mutants were hypersensitive to red light (Huq and Quail 2002) and that *AHL22*ox showed much more sensitive to red light either (Fig. 2A, B). As photoreceptor gene expression is largely unaffected by the over-expression of *AHL22*, we conclude that these factors lie upstream of *AHL22*, or that *AHL22* regulates hypocotyl growth via a mechanism independent of photoreceptor activity. Additional genetic and biochemical data are clearly needed to clarify the relationship between *AHL22*, *PIF* and *COP*.

The tissue-specific expression of *AHL22* relates to its function

AHL22 expression is more tissue-specific than either *AHL25* (*AGF1*) (seedlings, leaves, stems, floral tips, and flowers: Matsushita et al. 2007) or *AHL27* and *AHL29* (whole seedlings, Street et al. 2008). *AHL22* promoter is mainly active in the root hair zone and the hypocotyl-root transition zone (Fig. 5). The *AHL22*ox phenotype is much clearer with respect to flowering time and hypocotyl length, even though transcript abundance is greater in the roots than in the leaves and flowers of the wild type plants (Fig. 5). However, the level of *AHL22* transcript within a given tissue is in good correspondence with the strength of the phenotype—so for example, the higher the level of expression, the later the plant flowered (Fig. S1). Thus, *AHL22* appears to enhance vegetative growth and inhibit reproductive growth in a dosage-dependent manner.

The *ecc2* mutant, which is the initial material of this study, is an activation-tagging mutant in the background of *cry1 cry2* double mutant, so we tried to explain the relationship between *AHL22* and *CRY1* and/or *CRY2*. Because *cry1 cry2* mutant flowered too late, we firstly expressed *AHL22* in wild type plants and got three types of transgenic lines as shown in Fig. S1. Then we crossed type II into *cry2* mutant. Interestingly, F1 plants showed type I phenotype (late flowering and no seeds, data not shown), suggesting that *cry2* may enhance the phenotype of *AHL22*ox, even though *cry1* was heterozygous in F1 plants. However, it is needed further extensive evidence to elucidate the relationship between *AHL22* and *CRY1* and/or *CRY2*.

Acknowledgments Thanks to Drs. Bekir Ülker and Jane Parker for kindly providing pJawohl8-RNAi and pLeela vectors, and to Dr. Robert Koebner for his critical reading of the manuscript. This work was supported in part by the National ''863'' Program of China (2006AA10A111, 2006AA10Z107, and 2007AA10Z119), the National Key Basic Research '973' Program of China (2004CB1 17206), the Key Technology R & D Program (2007BAD59B02), National Science Foundation of China (30671245), National Institute of Health (GM56265), and UCLA faculty research and Sol Leshin BGU-UCLA Academic Cooperation programs.

References

Ahmad M, Cashmore AR (1993) HY4 gene of *A. thaliana* encodes a protein with characteristics of a blue-light photoreceptor. Nature 366:162–166. doi:10.1038/366162a0

Aravind L, Landsman D (1998) AT-hook motifs identified in a wide variety of DNA-binding proteins. Nucleic Acids Res 26:4413–4421. doi:10.1093/nar/26.19.4413

Bastow R, Dean C (2003) Plant sciences. Deciding when to flower. Science 302:1695–1696. doi:10.1126/science.1092862

Cattaruzzi G, Altamura S, Tessari MA, Rustighi A, Giancotti V, Pucillo C, Manfioletti G (2007) The second AT-hook of the architectural transcription factor HMGA2 is determinant for nuclear localization and function. Nucleic Acids Res 35:1751–1760. doi:10.1093/nar/gkl1106

Clough SJ, Bent AF (1998) Floral dip: a simplified method for Agrobacterium-mediated transformation of *Arabidopsis thaliana*. Plant J 16:735–743. doi:10.1046/j.1365-313x.1998.00343.x

Cutler SR, Ehrhardt DW, Griffitts JS, Somerville CR (2000) Random GFP:cDNA fusions enable visualization of subcellular structures in cells of Arabidopsis at a high frequency. Proc Natl Acad Sci USA 97:3718–3723. doi:10.1073/pnas.97.7.3718

El-Din El-Assal S, Alonso-Blanco C, Peeters AJ, Wagemaker C, Weller JL, Koornneef M (2003) The role of cryptochrome 2 in flowering in Arabidopsis. Plant Physiol 133:1504–1516. doi:10.1104/pp.103.029819

Ferrario S, Immink RG, Shchennikova A, Busscher-Lange J, Angenent GC (2003) The MADS box gene FBP2 is required for SEPALLATA function in petunia. Plant Cell 15:914–925. doi:10.1105/tpc.010280

Fujimoto S, Matsunaga S, Yonemura M, Uchiyama S, Azuma T, Fukui K (2004) Identification of a novel plant MAR DNA binding protein localized on chromosomal surfaces. Plant Mol Biol 56:225–239. doi:10.1007/s11103-004-3249-5

Grasser KD, Launholt D, Grasser M (2007a) High mobility group proteins of the plant HMGB family: dynamic chromatin modulators. Biochim Biophys Acta 1769:346–357

Grasser M, Christensen JM, Peterhansel C, Grasser KD (2007b) Basic and acidic regions flanking the HMG-box domain of maize HMGB1 and HMGB5 modulate the stimulatory effect on the DNA binding of transcription factor Dof2. Biochemistry 46:6375–6382. doi:10.1021/bi6024947

Guo H, Yang H, Mockler TC, Lin C (1998) Regulation of flowering time by Arabidopsis photoreceptors. Science 279:1360–1363. doi:10.1126/science.279.5355.1360

Harrer M, Luhrs H, Bustin M, Scheer U, Hock R (2004) Dynamic interaction of HMGA1a proteins with chromatin. J Cell Sci 117:3459–3471. doi:10.1242/jcs.01160

Huq E, Quail PH (2002) PIF4, a phytochrome-interacting bHLH factor, functions as a negative regulator of phytochrome B signaling in Arabidopsis. EMBO J 21:2441–2450. doi:10.1093/emboj/21.10.2441

Launholt D, Merkle T, Houben A, Schulz A, Grasser KD (2006) Arabidopsis chromatin-associated HMGA and HMGB use different nuclear targeting signals and display highly dynamic localization within the nucleus. Plant Cell 18:2904–2918. doi:10.1105/tpc.106.047274

LeClere S, Bartel B (2001) A library of Arabidopsis 35S-cDNA lines for identifying novel mutants. Plant Mol Biol 46:695–703. doi:10.1023/A:1011699722052

Lim PO, Kim Y, Breeze E, Koo JC, Woo HR, Ryu JS, Park DH, Beynon J, Tabrett A, Buchanan-Wollaston V, Nam HG (2007) Overexpression of a chromatin architecture-controlling AT-hook protein extends leaf longevity and increases the post-harvest storage life of plants. Plant J 52:1140–1153

Lin C, Ahmad M, Cashmore AR (1996) Arabidopsis cryptochrome 1 is a soluble protein mediating blue light-dependent regulation of plant growth and development. Plant J 10:893–902. doi:10.1046/j.1365-313X.1996.10050893.x

Lin C, Yang H, Guo H, Mockler T, Chen J, Cashmore AR (1998) Enhancement of blue-light sensitivity of Arabidopsis seedlings by a blue light receptor cryptochrome 2. Proc Natl Acad Sci USA 95:2686–2690. doi:10.1073/pnas.95.5.2686

Lu Q (2005) Seamless cloning and gene fusion. Trends Biotechnol 23:199–207. doi:10.1016/j.tibtech.2005.02.008

Martinez-Garcia JF, Quail PH (1999) The HMG-I/Y protein PF1 stimulates binding of the transcriptional activator GT-2 to the PHYA gene promoter. Plant J 18:173–183. doi:10.1046/j.1365-313X.1999.00440.x

Matsushita A, Furumoto T, Ishida S, Takahashi Y (2007) AGF1, an AT-hook protein, is necessary for the negative feedback of AtGA3ox1 encoding GA 3-oxidase. Plant Physiol 143:1152–1162. doi:10.1104/pp.106.093542

Mockler TC, Guo H, Yang H, Duong H, Lin C (1999) Antagonistic actions of Arabidopsis cryptochromes and phytochrome B in the regulation of floral induction. Development 126:2073–2082

Nagy F, Schafer E (2002) Phytochromes control photomorphogenesis by differentially regulated, interacting signaling pathways in higher plants. Annu Rev Plant Biol 53:329–355. doi:10.1146/annurev.arplant.53.100301.135302

Ni M, Tepperman JM, Quail PH (1998) PIF3, a phytochrome-interacting factor necessary for normal photoinduced signal transduction, is a novel basic helix-loop-helix protein. Cell 95:657–667. doi:10.1016/S0092-8674(00)81636-0

Ni M, Tepperman JM, Quail PH (1999) Binding of phytochrome B to its nuclear signalling partner PIF3 is reversibly induced by light. Nature 400:781–784. doi:10.1038/23500

Osterlund MT, Hardtke CS, Wei N, Deng XW (2000) Targeted destabilization of HY5 during light-regulated development of Arabidopsis. Nature 405:462–466. doi:10.1038/35013076

Pelaz S, Gustafson-Brown C, Kohalmi SE, Crosby WL, Yanofsky MF (2001) APETALA1 and SEPALLATA3 interact to promote flower development. Plant J 26:385–394. doi:10.1046/j.1365-313X.2001.2641042.x

Saijo Y, Sullivan JA, Wang H, Yang J, Shen Y, Rubio V, Ma L, Hoecker U, Deng XW (2003) The COP1-SPA1 interaction defines a critical step in phytochrome A-mediated regulation of HY5 activity. Genes Dev 17:2642–2647. doi:10.1101/gad.1122903

Sgarra R, Lee J, Tessari MA, Altamura S, Spolaore B, Giancotti V, Bedford MT, Manfioletti G (2006) The AT-hook of the chromatin architectural transcription factor high mobility group A1a is arginine-methylated by protein arginine methyltransferase 6. J Biol Chem 281:3764–3772. doi:10.1074/jbc.M510231200

Street IH, Shah PK, Smith AM, Avery N, Neff MM (2008) The AT-hook-containing proteins SOB3/AHL29 and ESC/AHL27 are negative modulators of hypocotyl growth in Arabidopsis. Plant J 54:1–14. doi:10.1111/j.1365-313X.2007.03393.x

Su Y, Kwon CS, Bezhani S, Huvermann B, Chen C, Peragine A, Kennedy JF, Wagner D (2006) The N-terminal ATPase AT-hook-containing region of the Arabidopsis chromatin-remodeling protein SPLAYED is sufficient for biological activity. Plant J 46:685–699. doi:10.1111/j.1365-313X.2006.02734.x

Sung S, Amasino RM (2004) Vernalization and epigenetics: how plants remember winter. Curr Opin Plant Biol 7:4–10. doi:10.1016/j.pbi.2003.11.010

Turck F, Fornara F, Coupland G (2008) Regulation and identity of florigen: flowering locus T moves center stage. Annu Rev Plant Biol 59:573–594. doi:10.1146/annurev.arplant.59.032607.092755

Ulm R, Baumann A, Oravecz A, Mate Z, Adam E, Oakeley EJ, Schafer E, Nagy F (2004) Genome-wide analysis of gene expression reveals function of the bZIP transcription factor HY5 in the UV-B response of Arabidopsis. Proc Natl Acad Sci USA 101:1397–1402. doi:10.1073/pnas.0308044100

Vom Endt D, Soares e Silva M, Kijne JW, Pasquali G, Memelink J (2007) Identification of a bipartite jasmonate-responsive promoter element in the *Catharanthus roseus* ORCA3 transcription factor gene that interacts specifically with AT-Hook DNA-binding proteins. Plant Physiol 144:1680–1689. doi:10.1104/pp.107.096115

Weigel D, Glazebrook J (2002) TAIL-PCR. In: Weigel D, Glazebrook J (eds) Arabidopsis, a laboratory manual. Cold Spring Harbor Laboratory Press, Cold Spring Harbor, pp 144–153

Weigel D, Ahn JH, Blazquez MA, Borevitz JO, Christensen SK, Fankhauser C, Ferrandiz C, Kardailsky I, Malancharuvil EJ, Neff MM, Nguyen JT, Sato S, Wang ZY, Xia Y, Dixon RA, Harrison MJ, Lamb CJ, Yanofsky MF, Chory J (2000) Activation tagging in Arabidopsis. Plant Physiol 122:1003–1013. doi:10.1104/pp.122.4.1003

Zhao X, Yu X, Foo E, Symons GM, Lopez J, Bendehakkalu KT, Xiang J, Weller JL, Liu X, Reid JB, Lin C (2007) A study of gibberellin homeostasis and cryptochrome-mediated blue light inhibition of hypocotyl elongation. Plant Physiol 145:106–118. doi:10.1104/pp.107.099838